The UV photolysis of hydrazoic acid

L. G. Piper, R. H. Krech, and R. L. Taylor[a)]

Physical Sciences Inc., Woburn, Massachusetts 01801
(Received 31 January 1980; accepted 9 April 1980)

The UV photolysis of HN_3 has been studied by observing the temporal decay in the number density of the $NH(a\,^1\Delta)$ product following photolysis and by observing the temporal behavior of the fluorescence from the secondary photolysis product NH_2 ($\tilde{A}\,^2A_1$), both as a function of HN_3 pressure. The HN_3 was photolyzed at $\lambda \approx 290$ nm by pulses from a frequency-doubled, flashlamp-pumped dye laser while the $NH(a\,^1\Delta)$ was probed by laser-induced fluorescence on the $NH(c\,^1\pi - a\,^1\Delta)$ band system at 324 nm using a frequency-doubled, nitrogen-pumped dye laser. The data are analyzed to obtain the rate constants $k_2 = 18\times10^{-11}$ cm^{3}molecule^{-1}s^{-1} for the reaction $NH(a\,^1\Delta) + HN_3 \rightarrow NH_2(\tilde{A}\,^2A_1) + N_3$ [Eq.(2)], and $k_4 = 9.3\times10^{-11}$ cm^{3}molecule^{-1}s^{-1} for the reaction $NH_2(\tilde{A}\,^2A_1) + HN_3 \rightarrow NH_2(\tilde{X}\,^2B_1) + HN_3$ [Eq.(4a)]$\rightarrow$ $NH_3 + N_3$ [Eq.(4b)].

I. INTRODUCTION

The photolysis of HN_3 has been studied for a number of years.[1–24] The early experiments of Beckman and Dickenson[1,2] showed that the primary photolytic mechanism was to produce NH and molecular nitrogen. Subsequent work by Thrush[3] essentially mapped out the sequence of reactions which lead to the overall decomposition products, nitrogen, ammonia, and some hydrogen. Recent work by Paur and Bair,[15–17] and especially by McDonald *et al.*[18–20] have indicated the state-specific steps in the photolytic decomposition. The NH radical produced in the primary photolysis is in the $a\,^1\Delta$ state.[12,15–22] This electronically excited NH radical reacts with HN_3 to produce NH_2 ($\tilde{A}\,^2A_1$) and N_3. NH_2 ($\tilde{A}\,^2A_1$) emits throughout the visible and near infrared producing the α bands of ammonia.[25–29] The N_3 radicals may recombine with another N_3 to yield electronically excited nitrogen[30] which may then further decompose the HN_3. This sequence of possible reactions is summarized below:

$$HN_3 + h\nu \rightarrow NH\ (a\,^1\Delta) + N_2 \quad \text{(Primary photolysis)} \tag{1}$$

$$HN\ (a\,^1\Delta) + HN_3 \xrightarrow{k_2} NH_2\ (\tilde{A}\,^2A_1) + N_3\ , \tag{2}$$

$$NH_2\ (\tilde{A}\,^2A_1) \xrightarrow{k_3} NH_2\ (\tilde{X}\,^2B_1) + h\nu\ (\alpha \text{ bands of ammonia}), \tag{3}$$

$$NH_2\ (\tilde{A}\,^2A_1) + HN_3 \xrightarrow{k_{4a}} NH_2\ (\tilde{X}\,^2B_1) + HN_3\ , \tag{4a}$$

$$\xrightarrow{k_{4b}} NH_3 + N_3\ , \tag{4b}$$

$$N_3 + N_3 \xrightarrow{k_5} N_2\ (B\,^3\Pi_g) + 2N_2\ (X)\ , \tag{5}$$

$$N_2\ (B\,^3\Pi_g) \xrightarrow{k_6} N_2\ (A\,^3\Sigma_u^+) + h\nu\ (\text{nitrogen } 1^+ \text{ bands})\ , \tag{6}$$

$$N_2\ (A\,^3\Sigma_u^+) + HN_3 \xrightarrow{k_7} NH\ (A\,^3\Pi) + 2N_2\ , \tag{7}$$

$$N_3 + HN_3 \xrightarrow{k_8} \text{products}\ . \tag{8}$$

In the above mechanism we have ignored a number of minor products such as H, N_3, and other electronic states of NH which are thought by some to be produced in the primary photolytic step. In addition, we have neglected other possible products from Reaction (2) such as NH ($X\,^3\Sigma$) which probably is formed to a small extent in Reaction (2) either from electronic quenching or chemical reaction. We will discuss some of these additional steps in Sec. IV.

Paur and Bair[15–17] followed the temporal history of NH ($a\,^1\Delta$), while McDonald *et al.*[15–20] measured the temporal profile of the NH_2 ($\tilde{A}\,^2A_1$) fluorescence. The kinetic analyses of both agree on a value $k_2 = 9.3\times10^{-11}$ cm^3 molecule^{-1} s^{-1}. In addition, the analysis of McDonald *et al.* gave $k_4 = 3.2\times10^{-10}$ cm^{3}molecule^{-1} s^{-1}.

We have studied the photolysis of HN_3 using two different techniques. In one set of experiments, the HN_3 was photolyzed at $\approx$ 285 nm by light from a doubled dye laser, and the density of the NH ($a\,^1\Delta$) products was probed as a function both of time after the photolysis pulse and of HN_3 number density by laser-induced fluorescence (LiF) using a second doubled dye laser tuned to the NH ($c\,^1\Pi - a\,^1\Delta$) system at 324 nm. These experiments allowed a direct determination of the rate constant k_2. In a second set of experiments in pure HN_3 at pressures between 18 and 1150 mTorr, the fluorescence of NH_2 ($\tilde{A}\,^2A_1$) was monitored as a function of time during and after the photolysis laser pulse. The temporal profiles *and* intensities in these latter experiments were analyzed to extract k_2, k_3, and k_4. Our results are at variance with those presented by Paur and Bair,[15–17] and McDonald *et al.*[18–20] Both of our experimental techniques give $k_2 = 1.8\times10^{-10}$ cm^{3}molecule^{-1}s^{-1}. The analysis of the NH_2 fluorescence traces gives $k_4 = 9.3\times10^{-11}$ cm^{3}molecule^{-1}s^{-1}. In Sec. IV we will discuss possible reasons for the discrepancy between our results and those of Paur and Bair and McDonald *et al.*

II. EXPERIMENTAL

The apparatus constructed for this experiment is shown schematically in Fig. 1; it has been described in detail elsewhere.[31] The cylindrical photolysis cell is fabricated from black-passivated stainless steel. The laser beams (photolysis and LiF) enter and exit the cell through sidearms which contain conical light baffles to reduce light scattering off the entrance and exit windows of the cell. The windows are Suprasil quartz and are set at Brewster's angle to further reduce scattered light.

The azide is photolyzed by pulses from a doubled dye laser which can be operated either single shot or repetitively pulsed at 0.5–20 Hz. Excited species produced in the photolysis are observed directly in emission or they can be probed via laser-induced fluorescence with pulses from a second dye laser which is triggered off

[a)] Present address: Research and Laser Technology, 6 Frank Street, Rockport, Mass. 01966.

 0021-9606/80/140791-10$01.00

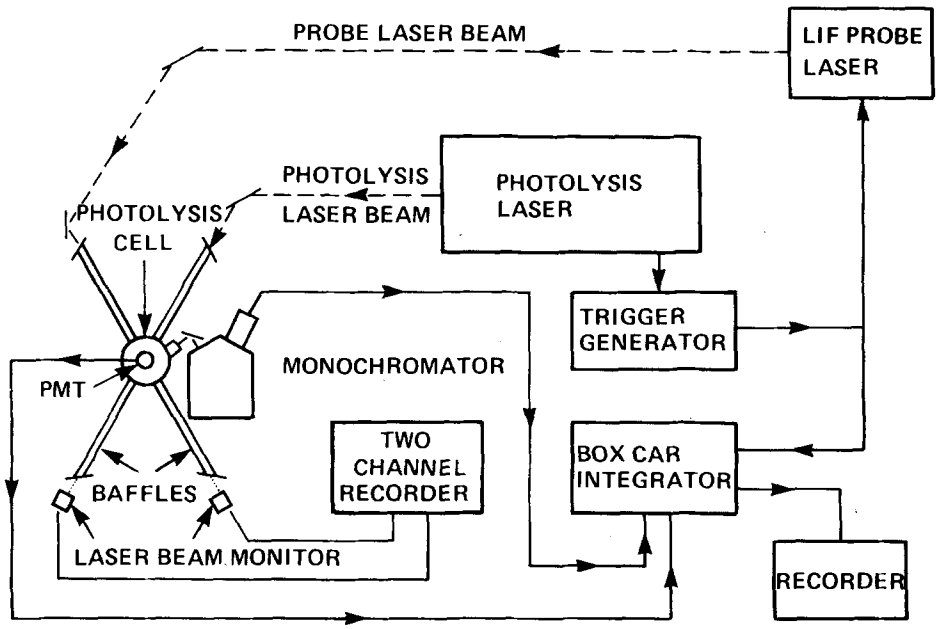

FIG. 1. Schematic of laser-photolysis apparatus.

the photolysis laser after a precisely controlled delay. Fluorescence is detected by a photomultiplier placed at right angles to the plane defined by the photolysis and probe lasers. In the single-shot mode, the output from the photomultiplier is monitored on an oscilloscope which is triggered off the photolysis laser. In the repetitive mode, the PMT signal voltage is fed into a boxcar integrator, the gate of which opens as the probe laser is fired. The gate is usually held open for a period of five fluorescent decays of the species of interest so that all fluorescence induced by the probe laser is collected. Interference filters are inserted between the reaction volume and the detector to reject scattered laser light and to provide spectral resolution. In repetitive experiments, the average intensities of the two lasers can be monitored to correct for long term drift. In the single-shot experiments, a quartz flat in the optical train of the photolysis laser directs about 15% of the laser's output into an energy meter for monitoring the laser energy on each shot. In addition, the photolysis-laser pulse is monitored with a fast photodiode, and its waveform is displayed on a second trace of the oscilloscope.

The two different photolysis lasers used in these studies were flashlamp-pumped dye lasers manufactured by Candela Corporation. The fundamental output of the laser was doubled using an angle-tuned KDP crystal. This provided UV outputs between 50 and 500 μJ per pulse of which about half was delivered by the optical train into the photolysis region. The photolysis laser was focused into the center of the cell with a Kepplerian telescope arrangement with a pinhole at the focus of the two telescope elements. The size of the photolysis-laser beam at its focus in the center of the cell is about 4 mm.

The laser used for the LiF probe was a Molectron DL-200, pumped by a 400 kW (UV14) nitrogen laser. The output of this laser was frequency doubled to 326 nm to probe the NH ($c\,^1\Pi$–$a\,^1\Delta$) system. The UV output from this laser was ≈ 1 μJ which was adequate to detect NH ($a\,^1\Delta$) number densities $\geq 10^7$–10^8 molecules cm^{-3}.

The optical detection system combines efficient light collection with good stray-light rejection, the latter from spatial filtering and the use of interference filters. Light from the interaction region is collected with a 50 mm diameter $f/1$ lens placed 50 mm from the interaction region. The parallel light rays exiting from the collection lens are refocused upon the photocathode of the photomultiplier with a 50 mm diameter $f/1.5$ lens placed immediately behind the collection lens. This system magnifies the image in the observation region about 1.5 times, thus giving a 31 mm diameter field of view in the cell when viewed with a 44 mm diameter photocathode. The f number for light collection of this system is about 1.24, giving a light collection efficiency of 4%. The collection system is very effective in reducing scattered light, since only a very restricted region of space within the photolysis cell is accessible to the detector. Further discrimination against scattered light is provided by the use of interference filters placed between the collection lenses and the photomultiplier.

In the laser-induced fluorescence studies, the detection system consisted of an EMI 9813 QA photomultiplier and an interference filter centered at 326 nm with a half-bandwidth of 10 nm. The NH_2 fluorescence was observed through a Corning CG 2-62 colored-glass filter (600 nm cutoff, long-pass filter) with an EMI 9659 QA photomultiplier, thus giving an effective spectral band-pass of 600–900 nm.

While the light collection system is efficient at collecting photons of interest and in rejecting stray light, it has the disadvantage of a restricted field of view which can degrade temporal information under some circumstances. At low pressures (in the mTorr range) the time required for a molecule to diffuse from the detec-

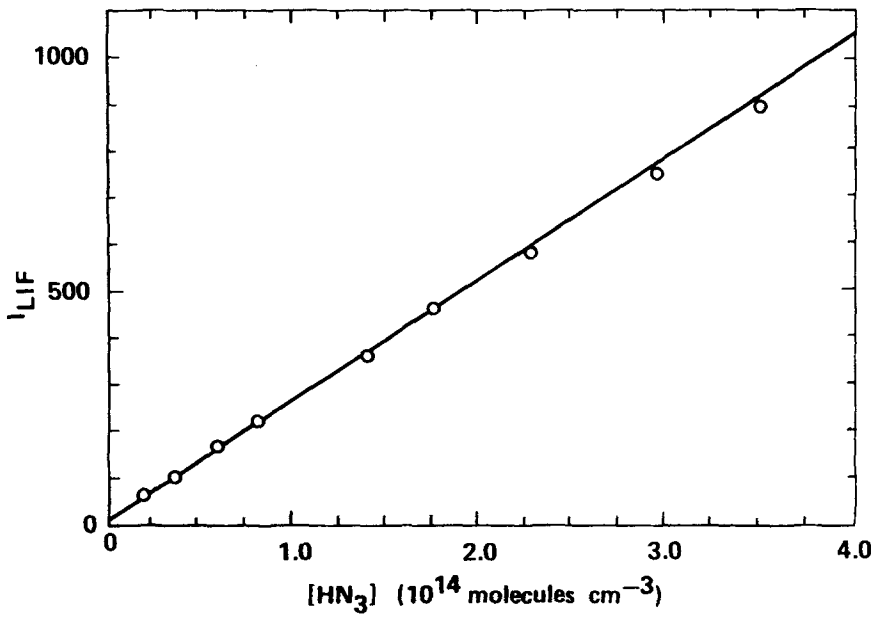

FIG. 2. Intensity of laser-induced fluorescence from NH ($a^1\Delta$) produced in HN_3 photolysis at 285 nm as a function of HN_3 number density. The data have been corrected for drift in photolysis- and probe-laser energy.

tor field of view can become short compared to molecular-fluorescence lifetimes or to chemical-reaction times. Diffusion may be slowed by using an inert buffer gas at high pressure, if quenching of the fluorescence by the buffer gas is not too significant. Quenching is small for most diatomic molecules even at pressures of a few hundred Torr; however, for polyatomic molecules such as NH_2 ($\tilde{A}\,^2A_1$),[32] quenching by the bath gas is significant, so that care must be taken to ensure that diffusive losses are not complicating kinetic measurements.

We modeled the diffusion of species out of our detector's field of view for the particular geometry of our system.[31] Two problems are created by diffusion: (i) the species of interest could diffuse out of the detector field of view prior to being observed, i.e., prior to fluorescing if the species emits radiation; (ii) those species detected by LiF could diffuse from the observation region prior to being probed by the LiF laser. The results of our modeling show that even at pressures as low as 30 mTorr, diffusion will have little effect (<10%) on temporal studies at times $\leq 40\mu$s. Our experimental observations of NH_2 ($\tilde{A}\,^2A_1$) fluorescence indicated that diffusion was not a serious problem even at pressures as low as 15 mTorr for times up to 50 μs.

The experiments using the LiF probe were done with the azide and argon buffer gas flowing slowly through the cell at total pressures of 5–50 Torr and HN_3 pressures of 0.3–20 mTorr. The reagents were introduced through calibrated flow meters, and the total cell pressure was measured by a pressure transducer (Validyne DP-7) which had been calibrated against oil and mercury manometers. The experiments in which the NH_2 ($\tilde{A}\,^2A_1$) fluorescence was monitored were done in a static cell using pure HN_3. The pressures were measured with a thermocouple gauge which had been calibrated against a pressure transducer using HN_3 as the calibration gas.

The HN_3 was synthesized by heating NaN_3 in excess stearic acid at temperatures of about 150 °C. The initial gas evolved in the synthesis was pumped away to reduce complications which might arise from volatile impurities either in the NaN_3 or the stearic acid.

III. RESULTS

A. Laser-induced fluorescence studies

In the experiments on the photolysis of HN_3 with the subsequent detection of NH ($a^1\Delta$) via LiF, the P_2–P_5 and Q_2–Q_8 lines of the NH ($c^1\Pi$ $v'=0 \rightarrow a^1\Delta$ $v''=0$) transition were positively identified via comparison with published spectra.[18,33] Figure 2 is a plot of the LiF intensity from the P_2/Q_5 lines at 325.9 nm as a function of $[HN_3]$. The finite intercept was the signal observed in the absence of added HN_3 and results from scattered light from the probe-laser pulse. The data were taken with a photolysis-laser energy of about 125 μJ and a probe-laser energy of about 0.5 μJ. Calculations based upon the known absorption coefficient of HN_3 at the photolysis wavelength[34] and the estimated photolysis laser beam energy and geometry indicate that at an HN_3 number density of 10^{14} molecules cm^{-3}, the number density of NH ($a^1\Delta$) produced (assuming a quantum yield of 1) should be $\approx 7\times10^9$ molecules cm^{-3}. The observed LiF signal under these conditions was 265 mV. Given a minimum detectable signal of ≈ 2 mV, the data indicate a detection limit of $\approx 5\times10^7$ molecules cm^{-3} for our LiF system. This is an upper limit since the quantum yield could be less than 1, and, in addition, the LiF laser was not optimized either for energy or linewidth.

The departure from linearity at the higher HN_3 concentrations seen in Fig. 2 probably results from removal of the NH ($a^1\Delta$) by NH_3, either via chemical reaction or electronic quenching during the period between the photolysis pulse and the probe pulse (about 2 μs), and some quenching of the NH ($c^1\Pi$) fluorescence by HN_3.

Analysis of oscilloscope traces of the NH ($c^1\Pi$,

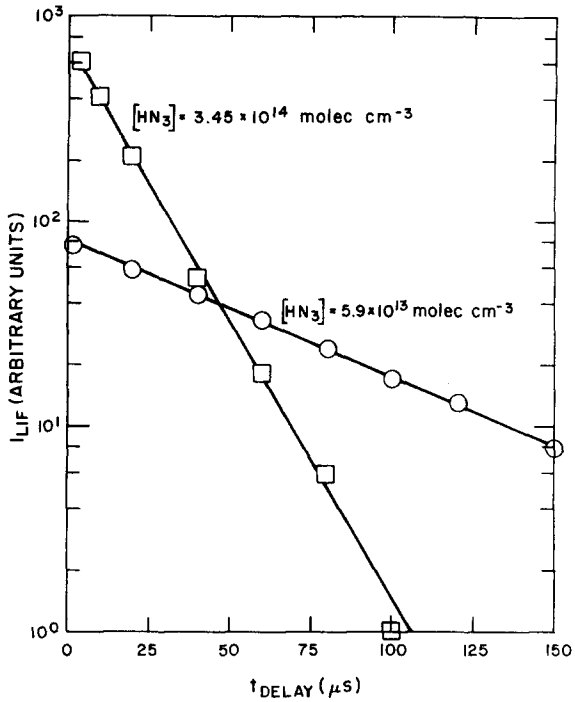

FIG. 3. Decay of NH ($a^1\Delta$) LIF intensity as a function of delay time between photolysis and probe lasers.

$v' = 0$) fluorescence decay indicates a lifetime of about 0.47 μs, within the range of reported values which are between 0.40 and 0.49 μs.[35–38]

For fixed $[HN_3]$, the NH ($a^1\Delta$) LiF intensity shows a first-order decay as the time between the photolysis and probe lasers is increased (Fig. 3). This results primarily from removal of the NH ($a^1\Delta$) by HN_3 [Reaction (2)]. After termination of the photolysis-laser pulse, the rate equation for the concentration of [NH ($a^1\Delta$)] with time is

$$\frac{d[\mathrm{NH}(a^1\Delta)]}{dt} = -k_2[\mathrm{NH}\ (a^1\Delta)][\mathrm{HN_3}] \ . \tag{9}$$

Under pseudo-first-order conditions ($[HN_3] \gg [NH\ (a^1\Delta)]$), the solution to this equation is

$$\ln \frac{[\mathrm{NH}\ (a^1\Delta)]}{[\mathrm{NH}\ (a^1\Delta)]_0} = -k_2[\mathrm{HN_3}]\, t \ . \tag{10}$$

Semilog plots of the concentration of NH ($a^1\Delta$) (or the LiF intensity which is directly proportional to that concentration) versus time will be linear with slopes equal to $-k_2[HN_3]$. Such linear plots are shown in Fig. 3. If several decay slopes are measured at varying values of $[HN_3]$, then a plot of the negative decay slopes versus $[HN_3]$ will give a straight line whose slope will be equal to k_2. Such a plot is shown in Fig. 4. The rate constant k_2 for the removal of NH ($a^1\Delta$) by HN_3 obtained from Fig. 4 is 1.7×10^{-10} cm^3 molecule^{-1} s^{-1}. This is about a factor of 2 larger than previously reported values,[17,20] but is a more direct determination than these measurements, and, furthermore, agrees with a detailed analysis of NH_2 ($\tilde{A}\,^2A_1$) fluorescence traces given below.

The finite intercept in Fig. 4 probably results from the quenching of NH ($a^1\Delta$) by the argon bath gas. The rate constant for that process, obtained by dividing the intercept in Fig. 4 by the argon number density, is 1.2×10^{-14} cm^3 molecule^{-1} s^{-1}.

B. Analysis of $NH_2(\tilde{A}\,^2A_1)$ fluorescence traces

The fluorescence observed when low pressures of pure HN_3 are photolyzed is due to emission from the NH_2 ($\tilde{A}\,^2A_1$) – NH_2 ($\tilde{X}\,^2B_1$) system, the α bands of ammonia, extending from about 450 nm to beyond 900 nm.[25–29] Typical oscilloscope traces of this fluorescence are shown in Figs. 5 and 6. The fluorescence traces were fit two different ways by least squares programs to a kinetic model incorporating Reactions (1)–(4).

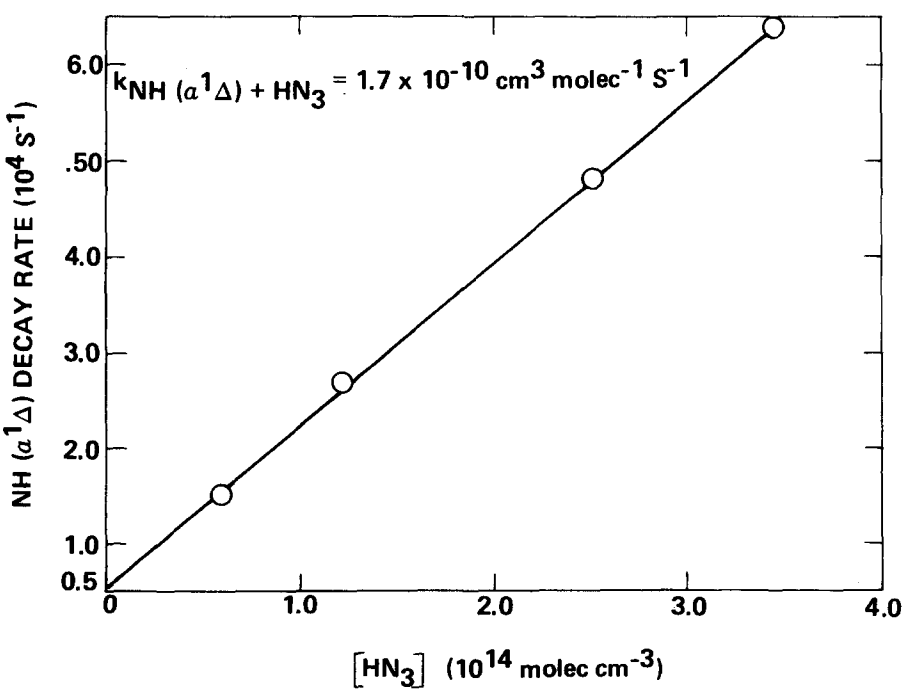

FIG. 4. Rate of decay of NH ($a^1\Delta$) as a function of $[HN_3]$ (argon pressure = 15 Torr).

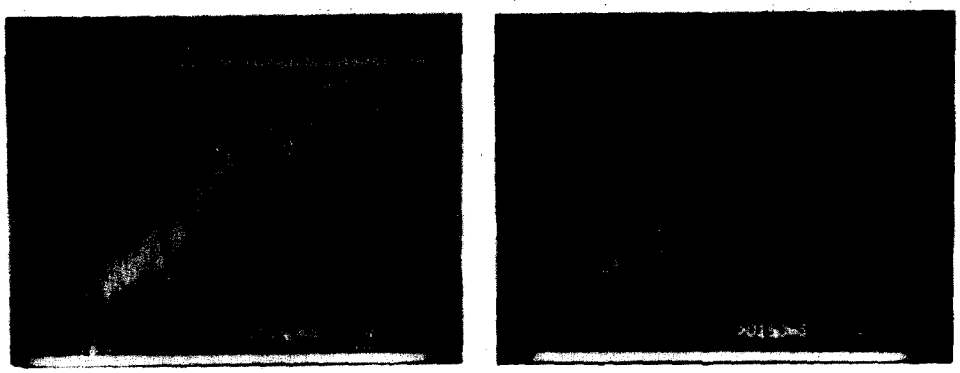

FIG. 5. Fluorescence from NH_2 ($\tilde{A}\,^2A_1$) following the photolysis of pure HN_3 at 295 nm. The solid lines over the oscilloscope traces are derived from the computer fitting procedure outlined in Sec. III. B.

The differential equation which describes the rate of change in [NH ($a\,^1\Delta$)], including production by the photolysis laser pulse, is

$$\frac{d[\mathrm{NH}\,(a^1\Delta)]}{dt} = k_1 I_{\mathrm{laser}}\, I(t)[\mathrm{HN_3}] - k_2[\mathrm{HN_3}][\mathrm{NH}\,(a^1\Delta)]\,, \tag{11}$$

where k_1 is a constant which includes the photolysis cross section, the laser beam cross-sectional area, photolysis quantum yield, and some appropriate conversion factors, the function $I(t)$ is the energy per unit time of the photolysis laser normalized to unit total energy, and I_{laser} is the total energy of the photolysis pulse. The rate equation for the concentration of NH_2 ($\tilde{A}\,^2A_1$) is

$$\frac{d[\mathrm{NH_2}\,(\tilde{A}^2A_1)]}{dt} = k_2[\mathrm{NH}\,(a^1\Delta)][\mathrm{HN_3}] - (k_3 + k_4[\mathrm{HN_3}]) \times[\mathrm{NH_2}\,(\tilde{A}^2A_1)]\,. \tag{12}$$

A Runge–Kutta numerical integration subroutine was written to solve the coupled differential equations (11) and (12) given values for the parameters k_1–k_4. The resulting number density of [NH_2 ($\tilde{A}\,^2A_1$)] was converted to a photon emission rate by multiplying by k_3 and another parameter ζ which incorporated such factors as collection system efficiency, effective PMT quantum efficiency, and the fraction of photons emitted outside the spectral bandpass of the system, i.e.,

$$I_{\mathrm{NH_2^*}}(t) = k_3\zeta[\mathrm{NH_2}\,(\tilde{A}^2A_1)](t)\,. \tag{13}$$

The Runge–Kutta subroutine for calculating [NH ($a\,^1\Delta$)], [NH_2 ($\tilde{A}\,^2A_1$)], and $I_{\mathrm{NH_2^*}}$ comprised the function subroutine in a nonlinear least squares program which fit 16 fluorescence traces covering the pressure range 18–1150 mTorr simultaneously to obtain a set of parameters k_1–k_4 and ζ which minimized the function

$$\chi^2 = \sum_{i=1}^{16}\sum_{j=1}^{n_i} (I_{ij}^{\mathrm{calc.}} - I_{ij}^{\mathrm{meas.}})^2\,. \tag{14}$$

The results of the fitting procedure gave $k_2 = 1.9\times10^{-10}$ cm^3 molecule^{-1} s^{-1}, $k_3 = 8\times10^4$ s^{-1} ($\tau_{eff} = 12.5$ μs), and $k_4 = 9.3\times10^{-11}$ cm^3 molecule^{-1} s^{-1}. Examples of the fits are shown as heavy lines over the traces in Fig. 5.

The value obtained for k_2 is in good agreement with the value obtained from the direct measurement of the decay of NH ($a\,^1\Delta$). The deduced value for k_3 yields an effective fluorescence lifetime for NH_2 ($\tilde{A}\,^2A_1$) of 12.5 μs, in agreement with the results of Halpern *et al.*[32] who measured values between about 7 and 25 μs for various vibronic levels of the NH_2 ($\tilde{A}\,^2A_1$) state. We should point out that our procedure fits not only the temporal profile of the fluorescence, but also the relative photon yield. The value obtained from the fit for k_1 agrees to within 20% with the value we would calculate assuming a quantum yield for Reaction (1) of unity. The 20% difference

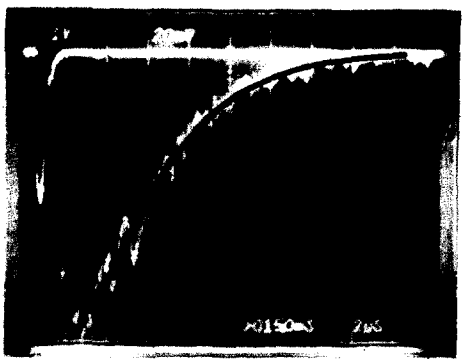

FIG. 6. Fluorescence from NH_2 ($\tilde{A}\,^2A_1$) following photolysis of pure HN_3 at 295 nm. The solid lines over the oscilloscope traces are derived from a computer fit using Eq. (17).

is less than the uncertainty in laser-beam energy and geometry in the observation region.

C. Alternative analysis of NH_2 ($\tilde{A}\,^2A_1$) for low-pressure data

At low pressures of HN_3, the duration of the NH_2 ($\tilde{A}\,^2A_1$) fluorescence trace is long compared to the duration of the photolysis pulse, e.g., at 120 mTorr the fluorescence extends for more than 15 μs while the FWHM pulse of our photolysis laser is 0.6 μs. Under these conditions, the first term in Eq. (11) may be neglected, and an analytical expression for $[NH_2\ (\tilde{A}\,^2A_1)]$ may be derived:

$$[NH_2\ (\tilde{A}\,^2A_1)] = \frac{k_3[HN_3][NH\ (a\,^1\Delta)]_0}{k_3 + k_4[HN_3] - k_2[HN_3]} \times \{\exp(-k_2[HN_3]t) - \exp[-(k_3 + k_4[HN_3])t]\}\ . \quad (15)$$

The intensity of the fluorescence from NH_2 ($\tilde{A}\,^2A_1$) is just k_3 (the radiative-decay rate constant) times the concentration of that species. The concentration of NH ($a\,^1\Delta$) at $t=0$ is given by

$$[NH\ (a\,^1\Delta)]_0 = k_1 I_{laser}[HN_3]\ . \quad (16)$$

Thus, the intensity of the NH_2 emission as a function of time is given by

$$I_{f1} = \frac{\gamma k_3 k_2[HN_3]^2 I_{laser}}{k_3 + k_4[HN_3] - k_2[HN_3]} \times \{\exp(-k_2[HN_3]t) - \exp[-(k_3 + k_4[HN_3])t]\}\ , \quad (17)$$

where γ is a constant which incorporates k_1 plus other experimental quantities such as effective photomultiplier quantum efficiency, the fraction of total emission occurring within the passband of the detection system, and optical-system collection efficiency. Eleven fluorescence traces taken at pressures between 27 and 112 mTorr were fit simultaneously to Eq. (17) using a nonlinear least squares routine to determine the parameters k_2, k_3, k_4, and γ. The computer-fit rate constants are $k_2 = 1.7\times10^{-10}$ cm^3 molecule^{-1} s^{-1}, $k_3 = 5.5\times10^{4}$ s^{-1} and $k_4 = 8.9\times10^{-11}$ cm^3 molecule^{-1} s^{-1}. These values are in good agreement with the rate constants obtained from the more complete treatment described in the previous subsection. Some fits of the fluorescence traces using this analytical procedure are shown in Fig. 6.

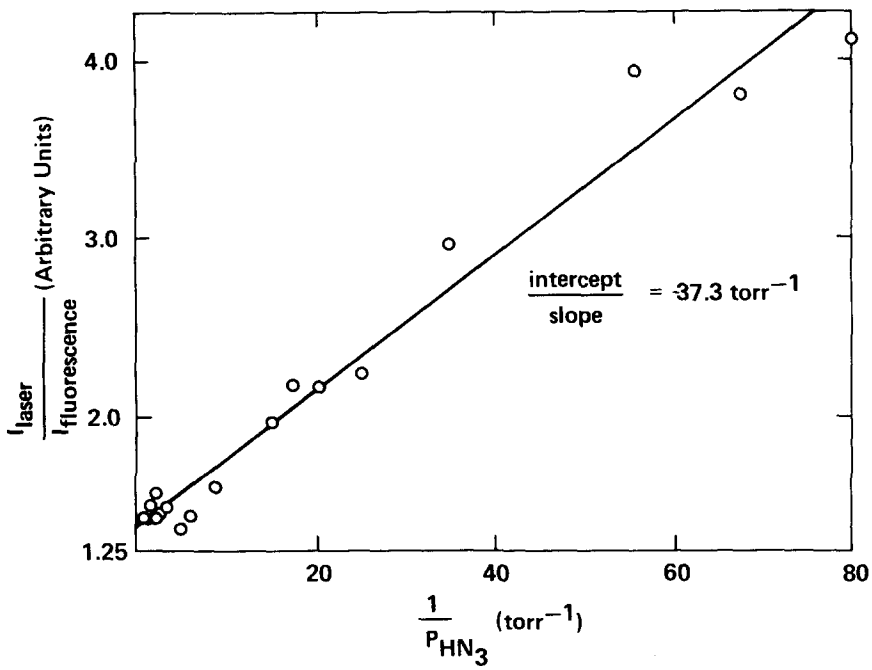

FIG. 7. The ratio of the laser energy to the total fluorescence from NH_2 ($\tilde{A}^2A_1$) following pure HN_3 photolysis at 295 nm as a function of the inverse HN_3 pressure. The ratio of the intercept to slope equals the ratio of the rate constant for removal of NH_2 ($\tilde{A}^2A_1$) by HN_3 to the effective radiative decay rate constant of NH_2 ($\tilde{A}^2A_1$).

D. Analysis of total fluorescence yields

The ratio k_4/k_3 may be determined directly from the data without resorting to computer fitting. Assuming that the total number of NH_2 ($\tilde{A}^2A_1$) radicals produced is some fraction (independent of pressure) of the NH ($a^1\Delta$) generated, and that losses in NH_2 ($\tilde{A}^2A_1$) occur only through fluorescence and quenching, a Stern–Volmer expression may be derived for the fluorescence yield of the NH_2 ($\tilde{A}^2A_1$):

$$I_{fl} = \frac{\zeta k_3[HN_3] I_{laser}}{k_3 + k_4[HN_3]} \quad . \tag{18}$$

This expression is also obtained by integrating Eq. (17) over time. Equation (18) may be rearranged and inverted to give

$$\frac{I_{laser}}{I_{fl}} = \frac{k_4}{\zeta k_3} + \frac{1}{\zeta[HN_3]} \quad . \tag{19}$$

Thus, a plot of the ratio of photolysis energy to the total fluorescence intensity versus the reciprocal of the HN_3 pressure should be linear, and the resulting ratio of the intercept to slope will be the ratio k_4/k_3. The data are plotted in this fashion in Fig. 7, and yield a k_4/k_3 of 37.3 Torr^{-1}, which is in good agreement with the ratio of 37.9 Torr^{-1} obtained from the computer fit to the fluorescence traces.

IV. DISCUSSION

A. Comparison with other experiments

The rate constants derived from our analyses differ considerably from those obtained by both McDonald *et al.*[20] and Paur and Bair.[15–17] We believe the graphical method of analysis used by McDonald *et al.*[20] will give values of k_2 which are too small and k_4 which are too large. The data of Paur and Bair[15–17] probably contain other sources of NH ($a^1\Delta$) in addition to direct photolysis which are active subsequent to the photolytic pulse. These are not accounted for in their data analysis, and this omission will cause their reported value for k_2 to be too small.

McDonald *et al.*[20] observed the temporal profiles of NH_2 ($\tilde{A}^2A_1$) fluorescence and analyzed them graphically using a model based upon Eq. (17). Equation (17) shows that the fluorescence trace is governed by a double exponential. The decay of the fluorescence trace is determined largely by the slower of the two exponentials while the faster exponential dominates the rise of the fluorescence. McDonald *et al.* plotted their data on semilog paper and took the slope of the tail of the fluorescence trace to be equal to the rate of the slower of the two exponentials. This identification is valid if the two exponential rates differ significantly and if the slope is taken sufficiently far out in the tail. They also extrapolated the decay slope back to zero time and took the slope (on the semilog plot) of the difference between the intensity from the decay extrapolation and the observed intensity to be the rate of the faster exponential. The procedure is demonstrated in Figs. 8 and 9 using fluorescence traces generated with our values for the rate

TABLE I. Rate constants for processes occurring following the UV photolysis of HN_3.

Process	Rate constant (10^{-11} cm^3 molecule^{-1} s^{-1})
$NH(a^1\Delta) + HN_3 \xrightarrow{k_2} NH_2(\tilde{A}^2A_1) + N_3$	18[a]
	9.3[b,c]
$NH_2(\tilde{A}^2A_1) + HN_3 \xrightarrow{k_{4a}} NH_2(\tilde{X}^2B_1) + NH_3$	9.3[a]
$\xrightarrow{k_{4b}} NH_3 + N_3$	32[b]

[a]This work.
[b]McDonald *et al.*, Ref. 20.
[c]Paur and Bair, Ref. 17.

constants (Table I). They determined the rate constants k_2 and k_4 from the slopes of Stern–Volmer plots of the slow and fast decay rates, respectively, extracted by the above procedure from a number of fluorescence traces spanning a range in pressure of 2–25 mTorr.

McDonald *et al.* apparently identified the slow decay component with the removal of NH ($a^1\Delta$) [Reaction (2)] and the fast decay component with the removal of the NH ($\tilde{A}^2A_1$) [Reactions (3) and (4)]. In the low pressure region in which they analyzed their data, this identification turns out to be correct. However, at pressures ≈ 25 mTorr, our kinetic analysis indicates that the rates for removal of NH ($a^1\Delta$) and NH_2 ($\tilde{A}^2A_1$) are equal, and at even higher pressures, the removal of NH ($a^1\Delta$) is the faster process. Over most of the pressure range studied by McDonald *et al.*, the rates of the two processes differ by less than a factor of 2.

This similarity in the rates for removal of NH ($a^1\Delta$) and NH_2 ($\tilde{A}^2A_1$) destroys the accuracy of determining decay rates from the tail of the fluorescence trace by graphical methods. The signal level will become too small before the decay rate of the trace approaches its asymptotic limit. For example, at 12 mTorr, the middle of the range studied by McDonald *et al.*, the slope of the log of the fluorescence intensity versus time does not approach within 10% of the decay rate of the slow component until 55 μs by which point the intensity has dropped to less than 10% of the peak intensity. Our simulations further indicate that even a 10% error in the decay slope leads to errors of greater than 30% in determining the rate of the fast component. The errors will always give decays which are too small and rises which are too large. This is the direction of the discrepancy between our results and those of McDonald *et al.*

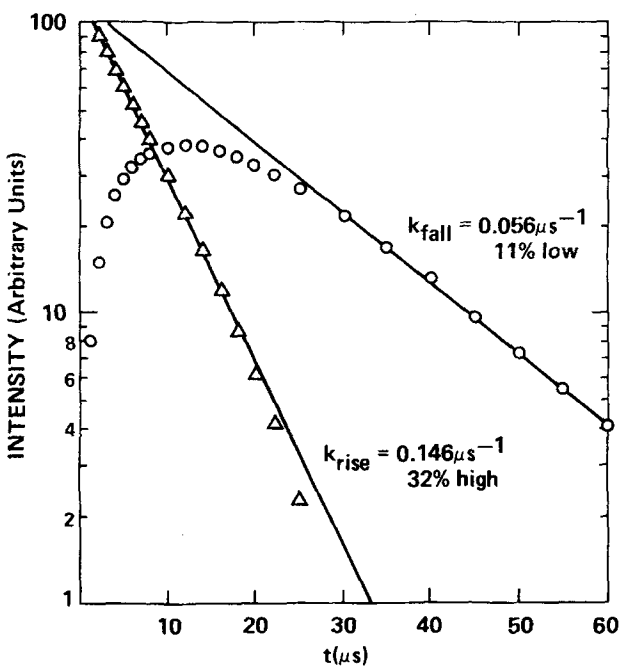

FIG. 8. Semilog plots of NH_2 ($\tilde{A}^2A_1$) fluorescence intensity as a function of time, following photolysis of pure HN_3 at 10 mTorr. The circles show the fluorescence trace which was generated from Eq. (17) using the rate constants k_2, k_3, and k_4 obtained from this study and listed in Table I. The triangles are generated from the difference between the limiting fluorescence-decay slope at late times and the actual fluorescence intensity. This figure illustrates the procedure used by McDonald *et al.*[20] to analyze their HN_3 photolysis data.

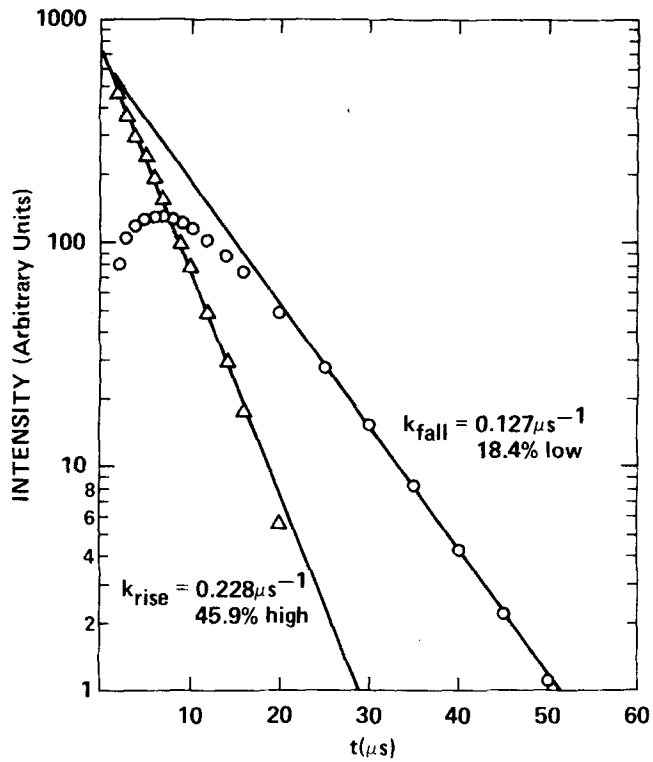

FIG. 9. The same as Fig. 8 except that the HN_3 pressure is 25 mTorr.

Paur and Bair[15–17] apparently derived the value they report for k_2 by computer simulation of the time history of the absorption of NH ($a^1\Delta$) during and after their photolysis flash. We think that the most likely source of error in the work of Paur and Bair is additional sources of NH ($a^1\Delta$) not included in their model. Production of NH ($a^1\Delta$) by other sources subsequent to photolysis will have the effect of slowing the observed NH ($a^1\Delta$) decay. Although Paur and Bair claim that their studies were done under isothermal conditions, it is clear from reading Paur's thesis,[15] upon which the work was based, that significant thermal decomposition took place in his apparatus at bath gas pressures below 20 Torr. The experiments they used for their kinetic analysis of k_2 were done at pressures of 2, 4, and 8 Torr of argon. In addition, they also observed some decomposition upon firing their flashlamps even when the lamps were covered by opaque foil.[15] This latter effect was thought to be due to electrical disturbances and prolonged the decomposition beyond the normal cutoff of the photolysis flash.

If nonisothermal conditions did exist in Paur and Bair's experiment, the issue must be addressed of whether thermal decomposition of HN_3 gives HN ($a^1\Delta$) as in photolytic decomposition or if, as some have suggested, it yields the ground state NH ($X^3\Sigma^-$). In his experi-

ments at low pressures ($\lesssim 2$ Torr) Gleu[39] observed emission from NH_2 ($\tilde{A}\,^2A_1$) during the thermal decomposition of HN_3 at temperatures ≈ 400 °C. This observation indicates that thermal decomposition does give NH ($a\,^1\Delta$) as a product which subsequently reacts with HN_3 to give the electronically excited NH_2 [Reaction (2)]. The reaction of NH ($X\,^3\Sigma^-$) with HN_3 is not sufficiently energetic to give electronically excited NH_2.[40] An additional indication that NH ($a\,^1\Delta$) is a product of the thermal decomposition of HN_3 comes from the IR multiphoton dissociation experiments of Hartford.[21] He observed NH_2 ($\tilde{A}\,^2A_1$) fluorescence when HN_3 was photolyzed at 10.6 μm. His observations are consistent with dissociation to form NH ($a\,^1\Delta$) followed by Reaction (2) to make the NH_2 ($\tilde{A}\,^2A_1$). On the other hand, in their shock-tube study, Kajimoto *et al.*[41] thought their data indicated that the thermal decomposition of HN_2 gave primarily NH ($X\,^3\Sigma^-$) since they failed to observe NH ($a\,^1\Delta$) with their absorption diagnostic. However, our measurement of k_2 indicates that even if the thermal decomposition of HN_3 gave only NH ($a\,^1\Delta$), it would be removed so rapidly by the HN_3, under the conditions of the experiment of Kajimoto *et al.*, as to preclude detection by them. Paur and Bair[15–17] have shown that some if not all of the NH ($X\,^3\Sigma^-$) formed in their system is produced by quenching of NH ($a\,^1\Delta$). Thus, we feel that, on balance, the evidence available suggests that the thermal decomposition of HN_3 like photolytic decomposition, gives significant amounts of NH ($a\,^1\Delta$), and that this additional source of NH ($a\,^1\Delta$) (which will be active after the photolytic pulse ends) is probably the major source of discrepancy between our results and those of Paur and Bair.

B. Minor photolytic processes

The photolytic decomposition mechanism outlined in Reactions (1)–(8) is by no means a complete description. We believe it encompasses the major processes, however. A few researchers have claimed that a minor channel in the primary photolysis produces atomic hydrogen and azide radicals directly[6,12,23]; however, this channel accounts for only a few percent at most of the primary photolytic decomposition. Other minor products which have been proposed to arise from primary photolysis are NH ($c\,^1\Pi$), NH ($A\,^3\Pi$), and NH ($X\,^3\Sigma^-$). The latter two products are spin forbidden at wavelengths longer than 120 and 188 nm, respectively, while NH ($c\,^1\Pi$) may be excited only by $\lambda \lesssim 210$ nm.[40] McDonald *et al.*[18] saw no evidence for the formation of triplet NH in their studies at 266 nm (the spin-forbidden thresholds are 294 and 2339 nm for the $^3\Pi$ and $^3\Sigma$ states, respectively).[40] In addition, Okabe[13] has shown that triplet NH formation is primarily a secondary process in the decomposition, being produced by processes such as Reaction (7).[42] Another source of triplet NH could be the electronic quenching of NH ($a\,^1\Delta$) to NH ($X\,^3\Sigma^-$) by the bath gas used in most studies. McDonald *et al.*[18] were not able to observe any triplet NH formation when helium was introduced into their system even at pressures as high as 90 Torr. However, the experiments of Paur and Bair[15–17] and of Stuhl[12] done with argon or nitrogen bath gas and our own direct observations of the decay of NH ($a\,^1\Delta$) in an argon bath tend to support such a quenching process. In all cases this quenching is minor, and observations show $[NH\,(X\,^3\Sigma^-)] \ll [NH\,(a\,^1\Delta)]$. In our computer analysis of the NH_2 ($A\,^2A_1$) fluorescence, electronic quenching of NH ($a\,^1\Delta$) was ignored. Our method of analysis would not be able to distinguish this quenching process from a reduced photolysis quantum efficiency. The good agreement with our computer-fit value for k_1, and that which would be calculated assuming a quantum yield of unity, indicates that direct quenching of NH ($a\,^1\Delta$) by HN_3 as opposed to Reaction (2) accounts for no more than $\approx 10\%$–20% of the removal of NH ($a\,^1\Delta$) by HN_3.

ACKNOWLEDGMENTS

This work was supported by the Department of Energy under contract number ES77-C-02-4223.A002. L. G. Piper wishes to acknowledge helpful discussions with W. Dimpfl and G. Arnold (Professor Kinsey's group at MIT), R. J. Cody (NASA/Goddard), J. R. McDonald and A. P. Baronavski (NRL), and D. R. Crosley (SRI International) during the construction phase of this work. The help of N.H. Kemp (PSI) on the analysis of diffusion effects was appreciated.

[1] A. O. Beckman and R. G. Dickinson, J. Am. Chem. Soc. 50, 1870 (1928).
[2] A. O. Beckman and R. G. Dickinson, J. Am. Chem. Soc. 52, 124 (1930).
[3] B. A. Thrush, Proc. R. Soc. (London) Ser. A 235, 143 (1956).
[4] E. D. Becker, G. C. Pimentel, and M. van Thiel, J. Chem. Phys. 26, 145 (1957).
[5] M. van Thiel and G. C. Pimentel, J. Chem. Phys. 32, 133 (1960).
[6] D. E. Milligan and M. E. Jacox, J. Chem. Phys. 41, 2838 (1964).
[7] J. A. R. Coope, J. B. Farmer, C. L. Gardner, and C. A. McDowell, J. Chem. Phys. 42, 2628 (1965).
[8] K. Rosengren and G. C. Pimentel, J. Chem. Phys. 43, 507 (1965).
[9] K. H. Welge, J. Chem. Phys. 45, 166 (1966).
[10] K. H. Welge, J. Chem. Phys. 45, 4374 (1966).
[11] P. H. H. Fischer, S. W. Charles, and C. A. McDowell, J. Chem. Phys. 46, 2162 (1967).
[12] F. Stuhl, dissertation, The University of Bonn, Bonn, Germany (1966).
[13] H. Okabe, J. Chem. Phys. 49, 2726 (1968).
[14] R. S. Konar, S. Matsumoto, and B. deB. Darwent, Trans. Faraday Soc. 67, 1698 (1971).
[15] R. J. Paur, Thesis, Indiana University (1973).
[16] R. J. Paur and E. J. Bair, J. Photochem. 1, 255 (1973).
[17] R. J. Paur and E. J. Bair, Int. J. Chem. Kinet. 8, 139 (1976).
[18] J. R. MCDonald, R. G. Miller, and A. P. Baronavski, Chem. Phys. Lett. 51, 57 (1977).
[19] A. P. Baronavski, R. G. Miller, and J. R. McDonald, Chem. Phys. 30, 119 (1978).
[20] J. R. McDonald, R. G. Miller, and A. P. Baronavski, Chem. Phys. 30, 133 (1978).
[21] A. Hartford, Jr., Chem. Phys. Lett. 57, 352 (1978).
[22] J. H. Smith and D. W. Robinson, J. Chem. Phys. 71, 271 (1979).
[23] P. L. Stepanov, V. M. Zamanskii, E. N. Moskvitina, and Yu Ya Kuzyakov, Vestn. Mosk. Univ. Khim. 14, 306 (1973).
[24] D. W. Cornell, R. S. Berry, and W. Lwowski, J. Am.

Chem. Soc. 88, 544 (1966).
[25]W. B. Rimmer, Proc. R. Soc. (London) 103, 696 (1923).
[26]A. Fowler and J. S. Badami, Proc. R. Soc. (London) 133, 325 (1931).
[27]G. Herzberg and D. A. Ramsay, Discuss. Faraday Soc. 14, 11 (1953).
[28]D. A. Ramsay, Mem. Soc. R. Sci. Liège Collect. 4 18, 471 (1957).
[29]J. W. C. Johns, D. A. Ramsay, and S. C. Ross, Can. J. Phys. 54, 1804 (1976).
[30]L. G. Piper, R. H. Krech, and R. L. Taylor, J. Chem. Phys. 71, 2099 (1979).
[31]L. G. Piper, R. H. Krech, and R. L. Taylor, "Investigation of Concept of Efficient Short Wavelength Laser," PSI TR-128 (1978), available from the authors on request.
[32]J. B. Halpern, G. Hancock, M. Lenzi, and K. H. Welge, J. Chem. Phys. 63, 4808 (1975).
[33]H. Gerzberg, *Molecular Spectra and Molecular Structure I. The Spectra of Diatomic Molecules* (Van Nostrand Reinhold, New York, 1950), p. 46.
[34]J. R. McDonald, J. W. Rabalais, and S. P. McGlynn, J. Chem. Phys. 52, 1332 (1970).
[35]W. H. Smith, J. Brzozowski, and P. Erman, J. Chem. Phys. 64, 4628 (1976).
[36]W. H. Smith, J. Chem. Phys. 51, 520 (1969).
[37]E. Fink and K. H. Welge, Z. Naturforsch. Teil A 19, 1193 (1964).
[38]D. Cvejanovic, A. Adams, and G. C. King, J. Phys. B 11, 1653 (1978).
[39]K. Gleu, Z. Phys. 38, 176 (1926).
[40]ΔH_f(NH) is taken from L. G. Piper, J. Chem. Phys. 70, 3417 (1979); ΔH_f(HN_3) is taken from C. Paillard, R. Moreau, and J. Combourieu, C. R. Acad. Sci. 264, 1721 (1967); ΔH_f(NH_2) is taken from JANAF Thermochemical Tables, Natl. Stand. Ref. Data Ser. Natl. Bur. Stand. 37 (1971); spectroscopic constants of NH are taken from J. M. Lents, J. Quant. Spectrosc. Radiat. Transfer 13, 297 (1973); and A. Gilles, J. Masanet, and C. Vermeil, Chem. Phys. Lett. 25, 346 (1974); and the spectroscopic constants of NH_2 are taken from Ref. 29.
[41]O. Kajimoto, T. Yamamoto, and T. Fueno, J. Phys. Chem. 83, 429 (1979).
[42]D. H. Stedman and D. W. Setser, Chem. Phys. Lett. 2, 542 (1968).